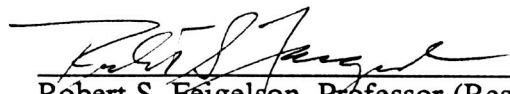


The Board of Trustees of the  
Leland Stanford Junior University  
Center for Materials Research  
Stanford, California 94305-4045  
Santa Clara, 12th Congressional District

Semi-Annual Technical Report  
on  
**PROTEIN CRYSTAL GROWTH IN LOW GRAVITY**  
NASA #NAG8-774  
CMR-89-9  
SPO#7218  
for the period  
April 27, 1989 through October 26, 1989

submitted to  
George C. Marshall Space Flight Center  
ES-76, Space Science Lab  
MSFC, AL 35812

Principal Investigator:

  
Robert S. Feigelson, Professor (Res.)  
Center for Materials Research  
Stanford, California 94305-4045  
(415) 723-4007

November 1989

## TABLE OF CONTENTS

	ABSTRACT	1
I.	INTRODUCTION	1
II.	FLUID FLOW	2
III.	ISOCITRATE LYASE	3
IV.	CONTROLLED NUCLEATION	5
V.	CONTROLLED NUCLEATION APPARATUS	5
VI.	REFERENCES	6
VII.	FIGURES	7



## ABSTRACT

This report covers the period of April 27 to October 26, 1989 for NASA Grant NAG 8-774. The objectives of and approach to the research is outlined. The further analysis of the flows around growing crystals is detailed. The preliminary study of the growth of isocitrate lyase and the crystal morphologies found are discussed. Preliminary results of controlled nucleation studies are presented.

### I. INTRODUCTION

The objective of this research is to study the effect of low gravity on the growth of protein crystals and those parameters which will affect growth and crystal quality. The proper design of the flight hardware and experimental protocols are highly dependent on understanding the factors which influence the nucleation and growth of crystals of biological macromolecules. Thus, the primary objective of this research is centered on investigating those factors and relating them to the body of knowledge which has been built up for "small molecule" crystallization. This data also provides a basis of comparison for the results obtained from low-g experiments.

The main component of this research program is the study of mechanisms involved in protein crystallization and those parameters which influence the growth process and crystalline perfection. Both canavalin and lysozyme are being used as the basic model proteins in these studies. Other biological macromolecules such as isocitrate lyase have been included in this research program when they provide an opportunity to better understand the nature of the crystallization process. The program involves four broad areas:

1. The application of both classical and novel chemical and physical techniques to study the fundamentals of protein crystallization. Included in this area are the study of the phase relationships in the systems of interest, primarily the factors controlling solubility, the study of growth kinetics to determine the growth rate controlling mechanism and the relevant activation energy involved in the process. The effects of fluid flow on the growth and perfection of protein crystals will be studied using flow visualization techniques. The use of electrochemical techniques to monitor and/or control crystallization will be studied also. The effects of applied voltages on nucleation and growth are not known nor is the magnitude of the potentials which may develop on the crystal during growth.

2. Characterization of protein crystals. Optical microscopy will give a general evaluation of crystal morphology, size and perfection. Phase contrast techniques will give enhanced contrast to the surface features allowing observation down to the  $0.1\mu$  level. For more detailed surface imaging the application of Scanning Tunneling Microscopy and Atomic Force Microscopy to protein crystals will be investigated. To study the defects occurring in the bulk of the crystals, the applicability of Synchrotron x-ray topography will be studied. The characterization studies will be attempting to associate the defects in protein crystals with the growth conditions to develop insights for growing crystals of greater perfection.
3. Control of nucleation and growth. The information developed in the phase relationship studies of section 1) will be used to design experiments to separately control the nucleation and growth processes. The information from section 2) will be used to optimize the growth.
4. The design and construction of a prototype of space flight hardware. The design will incorporate the results of section, 3) and will be instrumented to gather the types of data that have been acquired in the ground based studies.

## II. FLUID FLOW

The analysis of the flows around growing crystals has been expanded. In a previous report,<sup>(1)</sup> it was noted that flows had been observed around growing crystals of Rochelle salt, lysozyme and canavalin using the Schlieren imaging technique (Fig. 1). The values for the change of density and index of refraction with change of concentration for each system were also reported. The change in density and index of refraction with concentration do not by themselves indicate whether flow will occur and, if it does, whether that flow can be imaged. The Grashof number,

$$Gr = \frac{g\Delta\rho}{\rho v^2} L^3$$

(g is the acceleration of gravity,  $\Delta\rho$  the change in density across the diffusion boundary layer, L the characteristic length of the system-taken to be the height of the crystal,  $\rho$  the density and  $v$  the viscosity) is a non-dimensional, fluid dynamic variable that relates the buoyant force to the viscous drag. The larger this number, the more likely that flow will occur. More importantly, systems with the same Grashof number should behave alike. Thus, if a range of values of Grashof numbers can be established over which flow can be demonstrated to occur in crystallizing systems, then calculation of a Grashof number for a new system (macromolecular or not) will predict if flow should occur in that system.

Similarly, the ability to image the flow is not directly dependent on the change of index of refraction with concentration, but is related to the local change in light intensity

$$\Delta I/I = (f_2/a) \int (1/n) (\partial n/\partial x) dz$$

where  $f_2$  is the focal length of the second mirror in the schlieren optics,  $a$  the knife edge aperture,  $n$  the index of refraction,  $\partial n/\partial x$  is given by  $(dn/dc)(\partial c/\partial x)$  where  $x$  is the direction across the plume, and  $dz$  is perpendicular to the plan of the film. Again it should be possible to establish a range of values under which the flows will be visible. Comparisons of new systems will establish the possibility of flow visualization.

In addition to the values for the changes in density and index with concentration, it is necessary to establish the actual concentration at the crystal interface. For a crystal growing under diffusion control (Rochelle salt), it is equal to the solubility. However, lysozyme<sup>(2)</sup> and canavalin<sup>(3)</sup> grow under interface control and the interface concentration may be estimated by using a method outlined by Pusey and Naumann<sup>(4)</sup>. Using these estimates, the Grashof number and the local change in light intensity for each system have now been calculated under the experimental conditions. The values of the Grashof number are 772.48 for Rochelle salt, 23.04 for lysozyme and 67.84 for canavalin. If the Grashof number is normalized by fixing the size of the crystals at 1mm, then the Grashof numbers become 112.64 for Rochelle salt, 7.04 for lysozyme and 8.96 for canavalin. There is a much lower tendency for the protein solutions to experience convection under the conditions of these experiments even when size considerations are taken into account, but flow does occur in all these systems. The values found for the local change in intensity are 21.7 for Rochelle salt, 2.93 for lysozyme and 4.39 for canavalin. Based on the image quality of the films used in this study, the value of 2.39 appears to be near the limit of detectability in our system (400ASA film, f2.8, 1/51 sec exposure).

### III. ISOCITRATE LYASE

A study of the growth behavior of isocitrate lyase has recently begun. This is a joint project with Du Pont. When grown by the hanging drop method on earth, the crystal grows in a manner such that the corners grow out rapidly and the crystal quality is poor. Crystals grown in space however are equiaxed. Crystals of this material have been grown in our laboratory by the hanging drop method. The solutions used in this and subsequent growths were: a protein solution of 0.1ml of 13mg/ml isocitrate lyase with 0.004ml of a solution of 5.95mg of 3-nitropropionate and 107.23mg of magnesium acetate in 1ml of 50mM Tris (pH 7.0), and 0.004ml of a solution of 15.36mg of glutathione and 3.72mg of disodium EDTA in 0.15ml of 1M Tris (pH 8.0) (final protein concentration was 12mg/ml), and a well solution consisting of 72% saturated sodium citrate and containing 30mM Tris at

pH 8.3. The drop was made up of 2 $\mu$ l of the protein solution and 2  $\mu$ l of the well solution. The morphology of these crystals (Fig. 2 and 3) duplicates that of those produced at Du Pont. The growth rates were measured and, consistent with the morphology, the growth rate of the corners is initially high (1.8 microns/min) while that across the face center of the crystal is about 0.7 (Fig. 4 and 5). The growth rate of the corners remains above 0.2 microns/min for at least 1100 minutes while the face velocity drops essentially to 0 after 300 minutes. In order to test whether fluid flow was responsible for this unstable growth, a vapor equilibrium cell was built to allow flow visualization (Fig. 6). The cell volume was 20 $\mu$ l (5 times the volume of the 1-g hanging drop, 0.5 the volume of the space experiment). The cross section was 3mm x 1mm giving a surface area for equilibration which was 1/3 of that of the hanging drops. The crystals grown in this cell were equiaxed with a similarity to the space grown crystals (Fig. 7). No flow data has been collected yet.

Additional growth experiments have been conducted in 2mm diameter capillary tubes. In these experiments 10 $\mu$ l of protein solution and 10 $\mu$ l of well solution are placed in the capillary and equilibrated against the well solution in a larger tube attached to the capillary. These experiments have not duplicated the results of the the growth in the Schlieren cell, but crystals of two different morphologies were found (Fig. 8 and 9). A total of four different crystal morphologies have been seen in our laboratory. The predominant morphology observed has a cross section that appears to be a flattened hexagon. The end of the "hexagon" terminate in a wedge shape. This morphology is consistent with the orthorhombic symmetry of the isocitrate lyase unit cell ( $a=80.7\text{\AA}$ ,  $b=123.1\text{\AA}$  and  $c=183.4\text{\AA}$ )(5) with slow growing faces bounded by low index planes. A variation of this morphology was found in the crystals with the enhanced corner growth. The instability in growth occurs at the corners of the terminal faces of the "hexagonal" form.

The third morphology which was found were thin platelets of about 5m thickness. These platelets were four sided with apex angles of  $82.5\pm 1^\circ$  and  $98.1\pm 0.5^\circ$ . This morphology is not readily explained by the orthorhombic symmetry and low index slow growth planes. The final morphology observed was the equiaxed crystals previously mentioned. There is not enough information to completely describe their morphology.

Preliminary results show that the morphology of the isocitrate lyase crystals is not due to the sedimentation effect. Morphological stability seems to be related to the rate of equilibration of the protein solution and the crystal growth rate. Baird's work(6) shows that hanging drops equilibrate faster in 1-g than in space and the reduced surface area of the flow cell guarantees a slower equilibration. This is borne out by the lower nucleation and growth rates observed in the flow cell and the capillaries.

#### IV. CONTROLLED NUCLEATION

Preliminary controlled nucleation experiments using lysozyme have been conducted. These initial experiments used a small, temperature controlled spot to induce nucleation at a fixed position and to limit the number of nuclei produced. These experiments used lysozyme (20mg/ml, pH 4.0, 0.1M sodium acetate, and 4% sodium chloride). This solution will spontaneously nucleate in 4-5 days at room temperature. By using a cold spot temperature of 9°C, nucleation was accomplished in 5 hours. The number of nuclei was less when compared to the isothermal solutions, but they were not localized to the extent anticipated (Fig. 10).

#### V. CONTROLLED NUCLEATION APPARATUS

The results of the preliminary localized nucleation experiments has led to the design of the first prototype space flight hardware. This design incorporates a more sophisticated localized temperature gradient control as well as a means of controlling the ambient temperature around the growth cell as an aid to localizing the nucleation as well as a means of controlling subsequent growth. The apparatus also has provisions for in situ microscopy, the inclusion of Schlieren optics, and light scattering to detect the onset of nucleation (Fig. 11 and 12). This apparatus is currently under construction.

## VI. REFERENCES

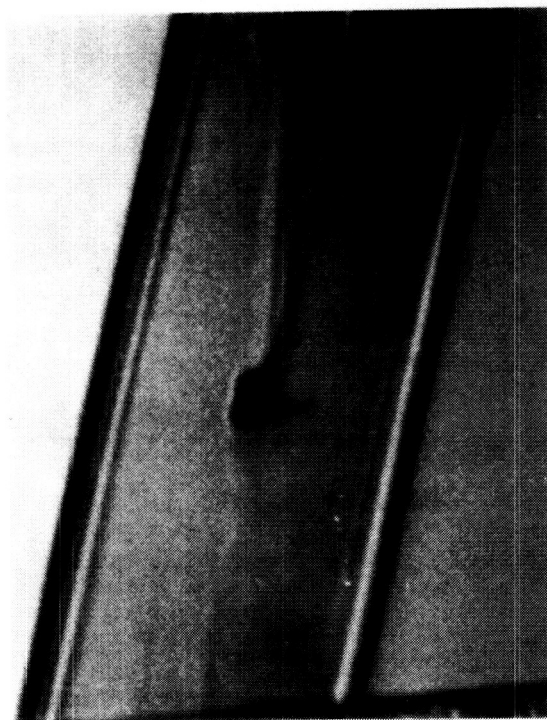
1. Final Report "Protein Crystal Growth in Low Gravity", NASA Grant NAG 8-489.
2. S. Durbin, Proceedings of Third International Conf. on the Crystallization of Biological Macromolecules, 13-19 August, 1989, Washington, D.C.
3. R. De Mattei and R. Feigelson, *J. Crystal Growth* 76, 333 (1989).
4. M. Pusey and R. Naumann, *J. Crystal Growth* 76, 593 (1986).
5. L. DeLucas, Private communication.
6. J. Baird with W. Fowles, L. DeLucas, P. Twigg, S. Howard and E. Meehan, *J. Crystal Growth* 90, 117 (1988), with L. Sibilie, proceedings of Third International Conf. on Crystallization of Biological Macromolecules, 13-19 August, 1989, Washington, D.C.

ORIGINAL PAGE  
BLACK AND WHITE PHOTOGRAPH

ORIGINAL PAGE  
BLACK AND WHITE PHOTOGRAPH

Rochelle Salt

Lysozyme



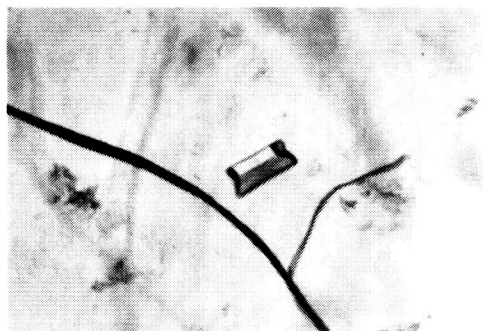
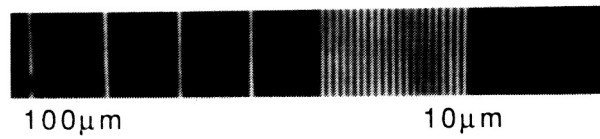
Canavalin

Pictures oriented with flows vertical.

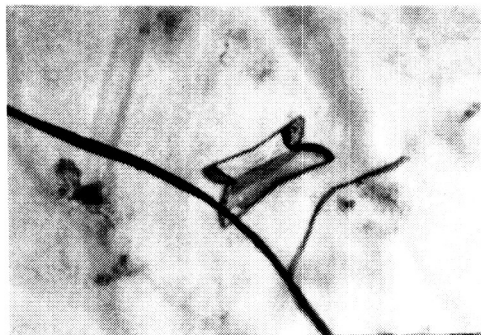
Fig. 1. Schlieren images of growth induced flow in Rochelle salt, lysozyme and canavalin.



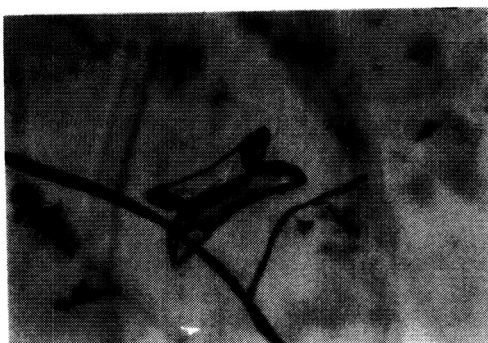
Isocitrate Lyase Crystal  
Grown by Hanging Drop Method  
Transmitted Light Microscopy  
150X



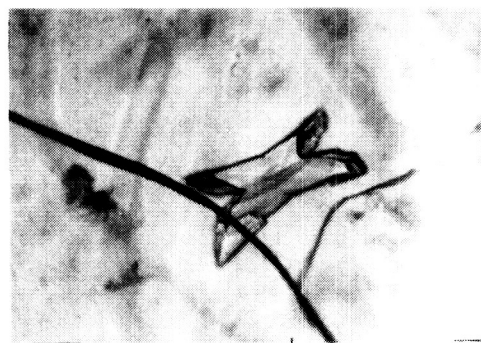
t = 0min



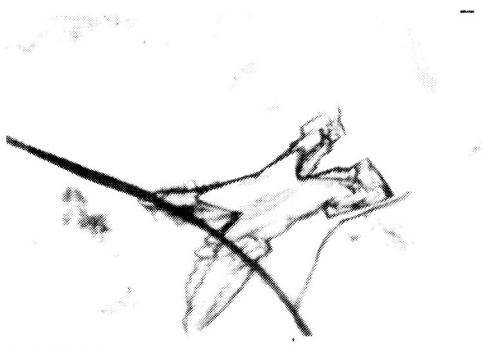
t = 94min



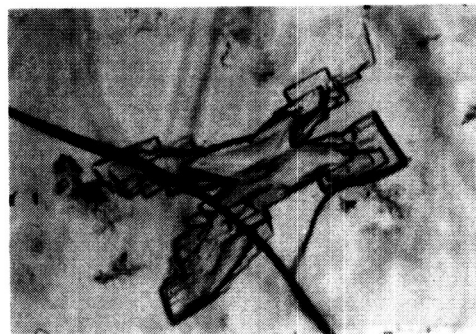
t = 143min



t = 200min



t = 1106min



t = 5568min

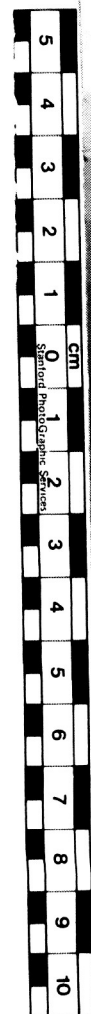


Fig. 2. Isocitrate lyase crystal grown by the hanging drop method at 1-g.

ORIGINAL PAGE  
BLACK AND WHITE PHOTOGRAPH

Isocitrate Lyase Crystal  
Grown by Hanging Drop Method  
Nomarski Microscopy

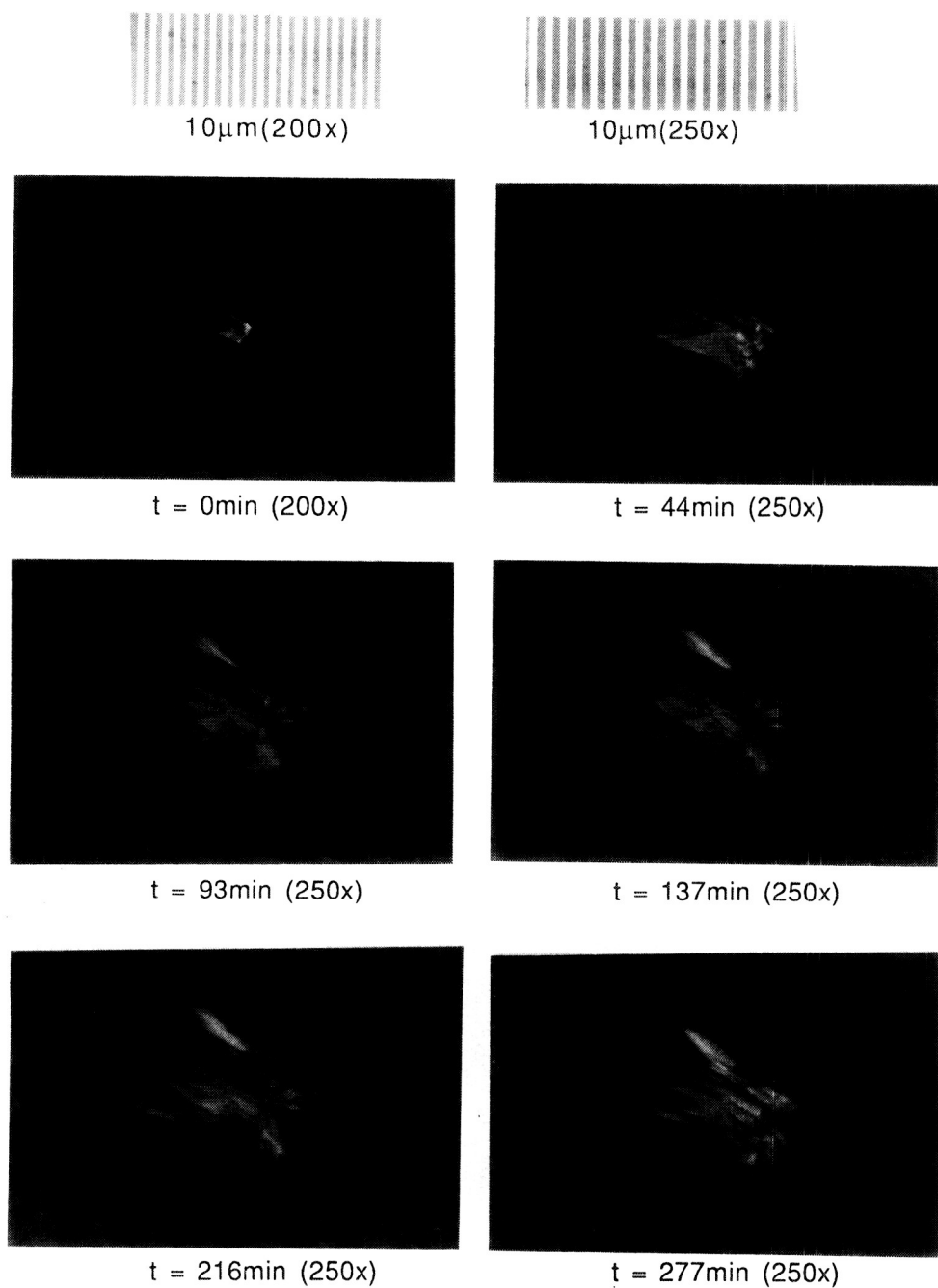
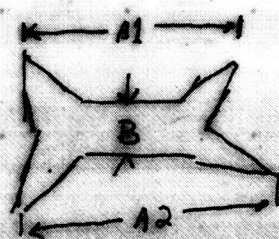


Fig. 3. Nomarski contrast micrographs of an isocitrate lyase crystal showing surface morphology.



# Isocitrate Lyase

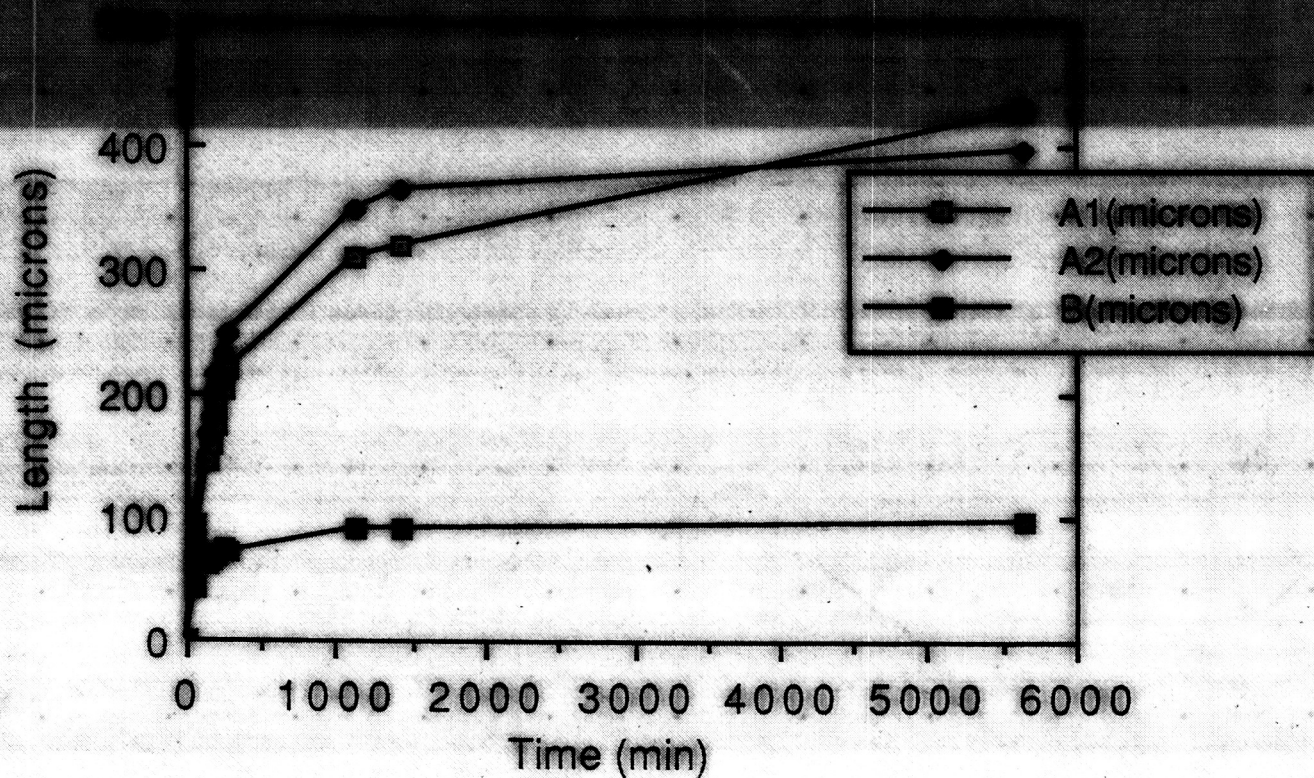


Fig. 4. Length versus growth time for crystal shown in Fig. 2.  $T=0$  is arbitrary.



# Isocitrate Lyase

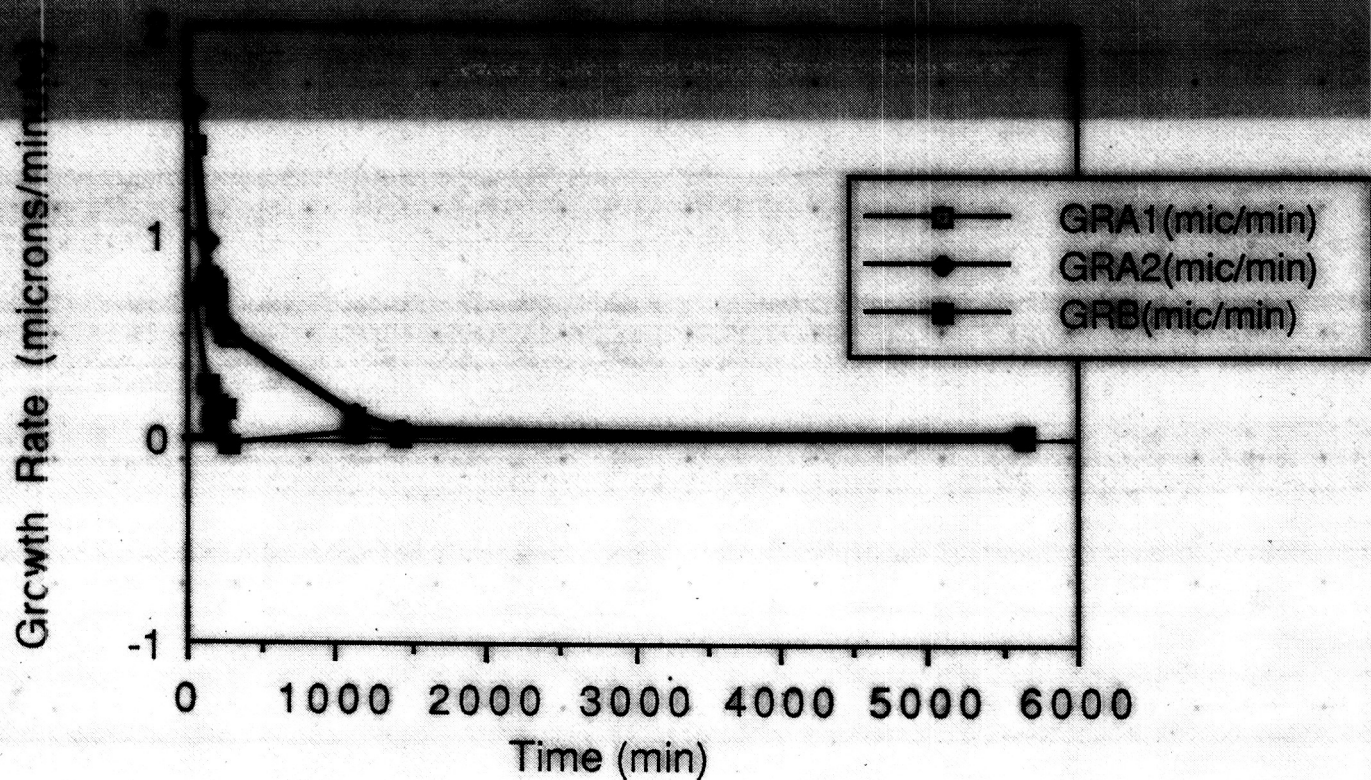


Fig. 5. Growth rate versus time for crystal shown in Fig. 2.

DOUBLE WELL VAPOR DIFFUSION CELL  
for  
PROTEIN CRYSTAL GROWTH

Design allows microscopy and flow imaging in growth well (left)

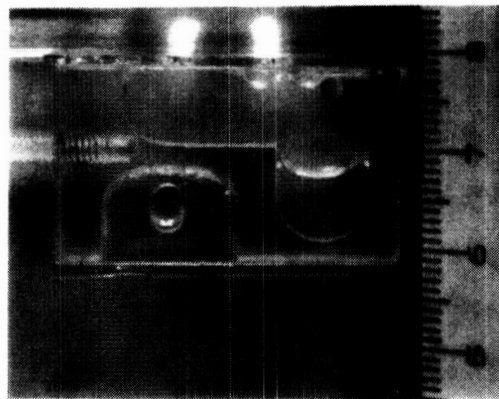


Fig. 6. Double well vapor diffusion cell.

ORIGINAL PAGE  
BLACK AND WHITE PHOTOGRAPH

ORIGINAL PAGE  
BLACK AND WHITE PHOTOGRAPH

Isocitrate Lyase Crystals  
Grown in Double Well Vapor Diffusion Cell  
Growth Time = 6.9 days (9924min)  
Transmitted Light Microscopy  
150X

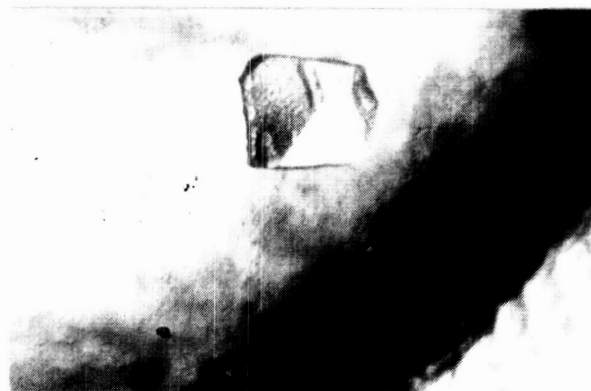


100μm

10μm



Grown near surface of solution



Grown near bottom of well

Fig. 7. Isocitrate lyase crystals grown in double well cell.



ORIGINAL PAGE  
BLACK AND WHITE PHOTOGRAPH



Fig. 8. Hexagonal-like isocitrate lyase crystals grown in capillaries.

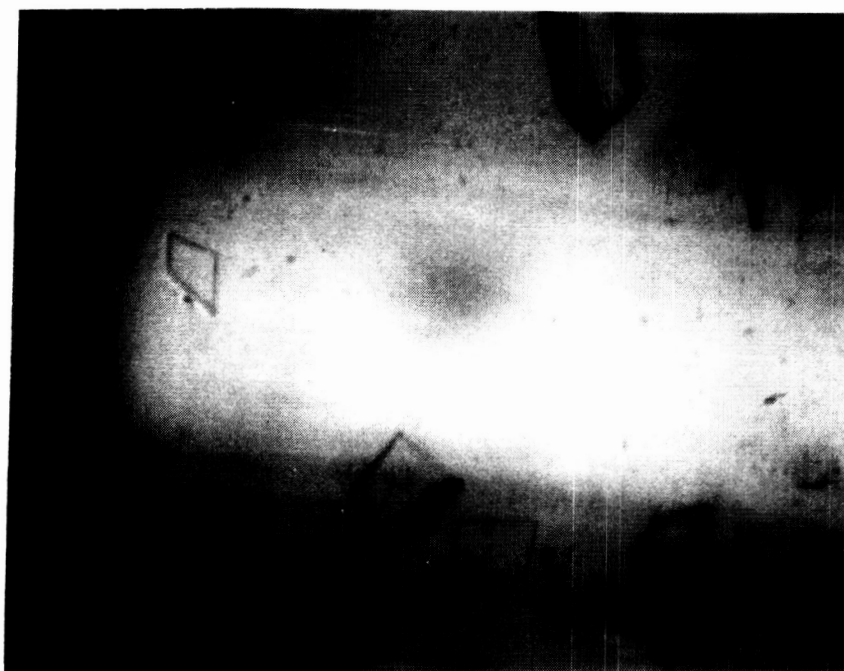
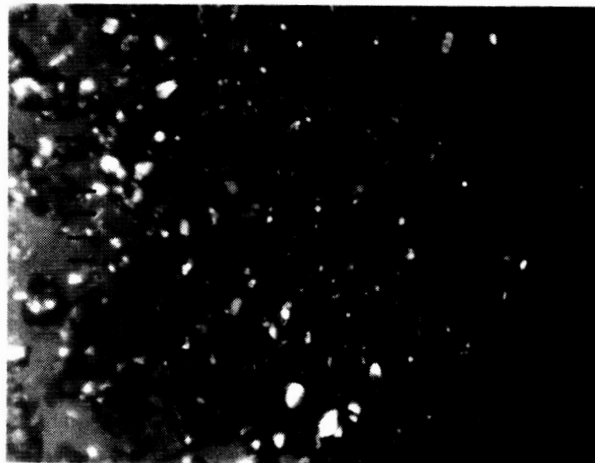


Fig. 9. Plate-like crystals of isocitrate lyase grown in capillaries.

ORIGINAL PAGE  
BLACK AND WHITE PHOTOGRAPH

UNCONTROLLED NUCLEATION



TEMPERATURE INDUCED  
NUCLEATION

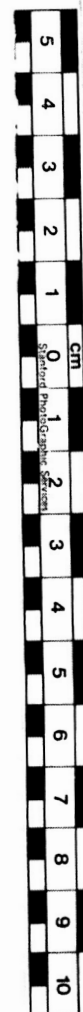


Fig. 10. Comparison of spontaneously nucleated and temperature nucleated lysozyme crystals. Index spacing is 100 $\mu$ .



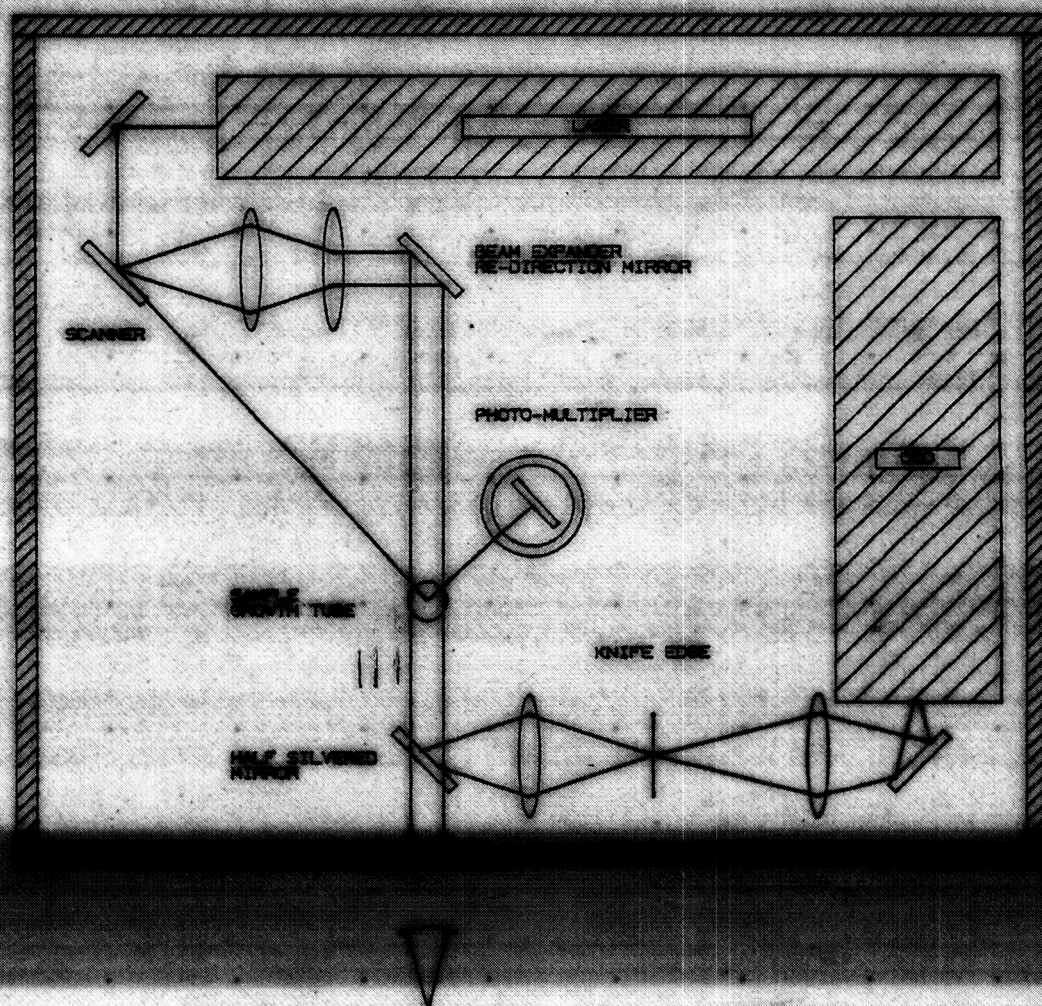
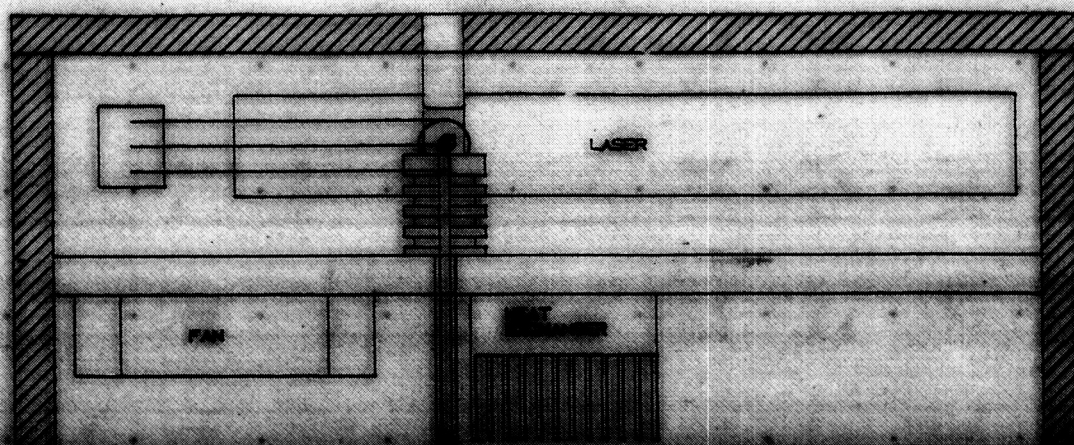


Fig. 11. Schematic drawing of controlled nucleation apparatus showing temperature controlled nucleation device, laser light source, fan and heat exchanger for overall temperature control, and optics for schlieren, light scattering and microscopy.



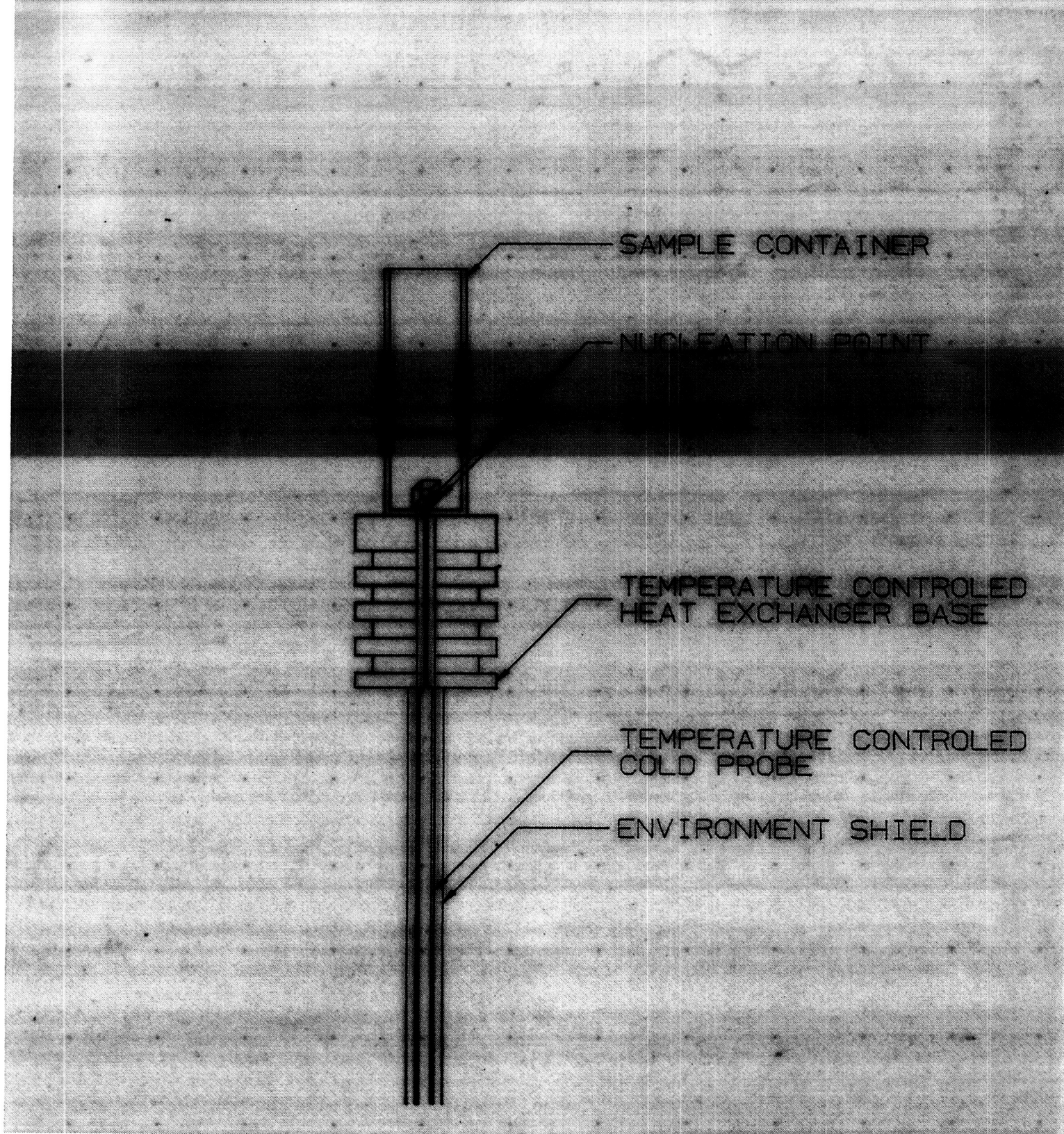


Fig. 12. Detail of temperature controlled nucleation device.